Int. J. Heat Mass Transfer. Vol. 33, No. 7, pp. 1451–1463, 1990
Printed in Great Britain

0017-9310/90 $3.00 + 0.00
Pergamon Press plc

Characterization of dryout in helical coils

GEORGES BERTHOUD and SREENIVAS JAYANTI†
Service des Transferts Thermiques, Centre d'Etudes Nucleaires de Grenoble, 85X-38041 Grenoble, France

(*Received* 3 *October* 1988 *and in final form* 22 *May* 1989)

Abstract—The prediction of the occurrence of dryout in helical coils is important for the proper design of the steam generators of some LMFBRs. Past work in this area is not satisfactory either in the prediction of the first dryout quality or in the treatment of the partial dryout region. Qualitative arguments are presented to show that dryout data can be classified into stratification-, redeposition- and entrainment-dominated dryout. Results obtained by various laboratories including experiments carried out at CENG, Grenoble, are used to develop transition criteria for these zones in a 'dryout map'. Correlations are given for dryout quality in each group. An analysis of the partial dryout region is also presented.

1. INTRODUCTION

WITH THE use of helical coiled steam generators in liquid metal-cooled nuclear reactors, the problems associated with dryout are receiving wide attention. Many studies have been conducted by various research teams [1–8] to investigate this phenomenon, and several correlations are available to predict the occurrence of dryout in helical coils. However, most of these correlations are not mechanism-based, and are valid only in a narrow range of the dynamic system parameters. The data of one team are not generally well predicted by the correlations of other teams. Also, despite the many studies on dryout in helical coils, it is still treated as a point transition, i.e. occurring at one axial position, whereas in practice a significant portion of the tube may be partially dried out.

Against this background, this paper has a two-fold purpose: to investigate systematically the nature of dryout in helical coils, and to characterize it quantitatively in such a way as to be of interest to the practising engineer. To this end, we present mechanism-based arguments to explain the observed influence of system parameters on dryout, and then use these arguments to correlate better a set of dryout data pooled from some publications available in the open literature. We also present a characterization of the partial dryout region, i.e. the length of tube in which the tube is only partially wetted, which can be used to develop a 'two-fluid' model in this region.

2. SPECIFICATION OF DRYOUT IN HELICAL COILS

In straight tubes, the transition from no dryout to total dryout of the tube occurs over a small length of tube, and hence it can be treated as a point transition under steady state conditions. However, in helical coils, this transition spreads over a considerable portion of the tube as shown schematically in Fig. 1. Thus, a complete specification of dryout in coils requires:

(a) the specification of the position—axial as well as circumferential—of the beginning of the dryout, say, in terms of thermodynamic quality;

(b) the propagation of the dryout front in the circumferential direction until the total dryout of the tube;

(c) the length of the region of partial dryout (which is important, but not readily calculable, in a temperature difference imposed system such as the steam generator of a liquid metal-cooled nuclear reactor);

(d) an estimate of the thermodynamic disequilibrium in this region.

In the present study, we address all these items except the last one. Inasmuch as the heat transfer between droplets of entrained liquid and the superheated vapour is high at high pressures [9], it is expected that the two phases will be close to a state of thermodynamic equilibrium. Moreover, the secondary flows in the vapour core of a coil bring the superheated vapour back into contact with the liquid film in the partial dryout region, and thus reduce the superheat. In view of these arguments, we make the assumption that the actual quality *in the partial dryout region* is about the same as the thermodynamic quality, and that the disequilibrium between the two phases in this region is negligible. This assumption must be kept in mind while using the correlations in the region of partial dryout of the coil.

3. FACTORS AFFECTING DRYOUT IN COILS

Following the analysis of dryout in straight tubes [10], we assume that the principal mechanism of dryout in helical coils is the disappearance of the liquid film near the wall as a result of thermo- and hydrodynamic effects. This being the case, a system par-

† Present address: Imperial College of London.

NOMENCLATURE

A	heat transfer area [m^2]
C, c_1	constants
D	coil diameter [m]
d	tube inside diameter [m]
d^*	modified tube diameter [m]
f_{nw}	fraction of non-wetted perimeter
f_w	fraction of wetted perimeter
G	mass flux, or mass velocity [kg m^{-2} s^{-1}]
g	acceleration due to gravity, 9.806 m s^{-2}
h	heat transfer coefficient [W m^{-2} K^{-1}]
P	pressure [bar]
Q	total heat transferred in the partial dryout region [W]
q''	heat flux [W m^{-2}]
Re	Reynolds number
T	temperature [K or °C]
x	thermodynamic quality
x_1	quality at the onset of dryout
x_{tot}	quality at the total dryout of the tube
δx	normalized quality in the partial dryout region
x_0	x-coordinate of the 'correlation map', $G/(\rho_v\sqrt{(gD)})$
y_0	y-coordinate of the 'correlation map', Gd^*/μ_l
z	position along the tube axis [m]
z_1	distance from a reference to the point of onset of dryout
z_{tot}	distance from the same reference to the point of total dryout
Δz	length of the partial dryout region, $z_{tot}-z_1$ [m].

Greek symbols

θ	angular position [deg]
λ	latent heat vaporization [J kg^{-1}]
μ	viscosity
ρ	density [kg m^{-3}]
σ	surface tension [N m^{-1}].

Subscripts

c	conduction in the tube wall
i	inside the tube
l	liquid phase
nw	non-wetted portion of the tube
o	outside the tube
pw	partial dryout region
sat	saturated condition of the fluid
v	vapour phase
w	wetted portion of the tube.

ameter can have an effect on dryout only if it can affect the local film thickness through some mechanism(s). Also, its influence on dryout can be predicted by systematically examining its effect on these mechanisms. This section is concerned with the identification of such factors.

A close inspection of the two-phase annular flow in helical coils reveals that there are four mechanisms through which the local film thickness can change:

(i) entrainment of liquid in the form of droplets;

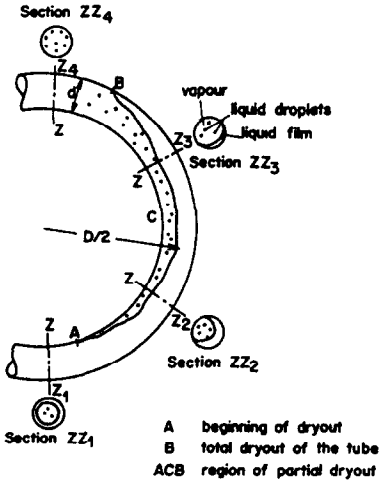

FIG. 1. Dryout in helical coils.

(ii) redeposition of these droplets;

(iii) phase change;

(iv) redistribution of the liquid film caused, among others, by the secondary flows.

Unlike in the case of two-phase annular flow in vertical tubes, these processes are not axisymmetric in helical coils. For example, the entrainment process depends on the film thickness, and thus may vary greatly in the azimuthal direction. Similarly, the redeposition of the droplets, which is influenced by gravitational and centrifugal forces, has a preferential direction; it will be more on the outer side (see Figs. 1 and 2 for the terminology used in this paper) than on the inner side of the tube. The role of secondary flow in two-phase flow in helical coils is not entirely clear. It is well-established (see, for instance, ref. [11]) that the secondary flows in a single-phase flow are created by the radial pressure gradient induced by the centrifugal force. In two-phase annular flow, the vapour core is continuous, and one can expect a double-vortex system of secondary flows to be present in the vapour core. In the liquid phase such a flow cannot exist, unless the liquid flow path is completed by a stream of entrained droplets going from the inner side to the outer side. This can happen only if the entrainment rate is much higher on the inner side. However, the secondary flow is very small in magnitude compared to the main axial flow [11], and should not cause much entrainment by itself. More-

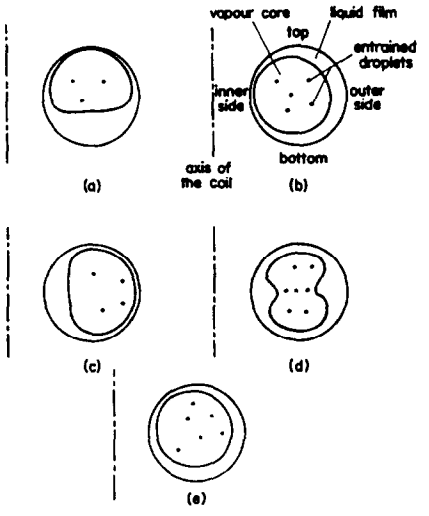

FIG. 2. Some possible forms of the variation of film thickness in two-phase annular flow in helical coils. (e) shows the most probable variation of film thickness at high pressures.

over, the shear stress of the gas phase on the wall (or the film in annular flow) is less on the inner side, and, at high relative pressures, the film on the inner side is thinner, as will be shown below. Thus it is unlikely that there is a stream of entrained droplets across the tube from the inner to the outer side, but one would expect the secondary flow in the vapour core to drag the top layers of the liquid film from the outer side to the inner side, making the flow less stratified (or more, in the case of 'inverted annular flow' in coils, see below). In this study, we assume that this is the principal mechanism of the redistribution of film flow in helical coils.

Since dryout occurs when the local film disappears, the distribution of the liquid phase in coils is very important as far as dryout is concerned. Unlike in straight vertical tubes, the film thickness varies around the circumference, and consequently, dryout in coils may begin earlier than in vertical tubes, although the average dryout quality is generally higher. Depending on the relative strength of the mechanisms cited above, the variation of film thickness around the tube may take any of the forms shown in Fig. 2. When the gravitational force on the flow is the predominant one, e.g. for large coil diameters and low mass fluxes, the flow may be stratified as in a horizontal tube (Fig. 2(a)). If the centrifugal force is very large, the film thickness may vary as shown in Fig. 2(b) if it is more on the liquid phase, or as in Fig. 2(c) if it is more on the vapour phase. The flow in Fig. 2(c) is generally called 'inverted annular flow' [12] in helical coils. The distribution in Fig. 2(d) is possible if centrifugal force-induced entrainment and redeposition overshadow other effects, although such local peaks in the film thickness have not been observed, and are not expected because the secondary flow is weak compared to the primary flow.

The distribution of film thickness at high relative

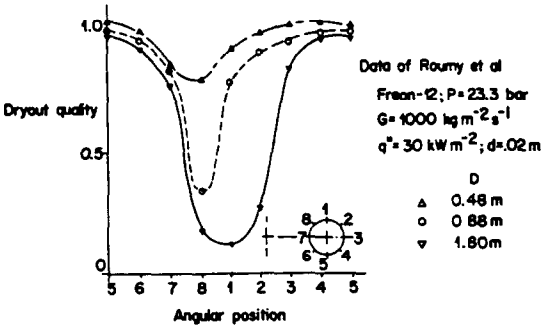

FIG. 3. Circumferential propagation of the dryout front in terms of local thermodynamic quality.

pressures encountered, for example, in power plants, seems to be as shown in Fig. 2(a) or (e), the former occurring at low mass fluxes. This distribution can be deduced from the spread (propagation) of partial dryout, which has been measured experimentally by many researchers. A typical result is shown in Fig. 3. Here, the wall temperature of a uniformly-heated helical tube was measured at regular intervals in the axial and circumferential directions [1]. The position (in terms of thermodynamic quality) of local dryout of the tube was detected by a sudden and sustained increase in the wall temperature at the point. We see that dryout begins between the inner and the upper side of the tube, and spreads almost symmetrically to the outer side. Since the occurrence of dryout corresponds to the disappearance of liquid film, these results lead us to the film thickness distribution shown in Fig. 2(e). We shall quantify these results later to estimate the angular position of the first dryout.

4. INFLUENCE OF SYSTEM PARAMETERS ON FIRST DRYOUT

The first dryout quality in coils has been shown to be very sensitive to system parameters such as mass flux and coil diameters, and sometimes contradictory effects have been reported (see ref. [2]), for example, that an increase in the mass flux increases and decreases the dryout quality. In this section, we deduce the influence of a system parameter on the position of first dryout by superposing its effect on each of the four mechanisms which affect the film thickness at a given point. In view of the fact that these mechanisms are not very well understood in helical coils, we consider only first-order influences, and neglect any second-order effects. We designate the position of dryout by the local thermodynamic (equilibrium) quality which is dimensionless and can easily be calculated. We investigate the effect of the following five parameters: inlet subcooling, pressure, coil diameter, heat flux and mass velocity, and present experimental evidence wherever available.

4.1. *Influence of inlet subcooling*

The inlet subcooling has no direct and major effect on any of the four mechanisms. Hence the first dryout

Table 1. Influence of inlet enthalpy on the first dryout quality (compiled from the experimental data of Unal [4]: working fluid, water; tube diameter, 0.018 m)

No.	P (bar)	D (m)	G (kg m^{-2} s^{-1})	q'' (kW m^{-2})	Subcooling T (°C)	x_{eq}	x_1
1	150	1.5	639	272	82	−0.71	0.31
2	150	1.5	635	270	42	−0.36	0.29
3	150	0.7	1206	554	128	−1.09	0.70
4	150	0.7	1200	548	72	−0.62	0.71
5	177	1.5	937	290	135	−2.11	0.60
6	177	1.5	892	288	90	−1.41	0.59
7	177	1.5	1272	358	136	−2.12	0.32
8	177	1.5	1236	346	58	−0.91	0.28
9	177	0.7	630	259	143	−2.23	0.54
10	177	0.7	636	257	95	−1.48	0.55
11	177	0.7	1224	487	137	−2.14	0.60
12	177	0.7	1234	468	97	−1.51	0.59
13	200	0.7	618	226	155	−4.63	0.28
14	200	0.7	616	216	106	−3.16	0.28
15	200	0.7	616	187	157	−4.67	0.35
16	200	0.7	623	186	106	−3.16	0.30
17	200	0.7	1236	341	151	−4.51	0.31
18	200	0.7	1227	340	96	−2.87	0.29
19	200	0.7	1491	401	143	−4.27	0.33
20	200	0.7	1498	393	98	−2.93	0.33
21	200	0.7	1500	385	97	−2.88	0.43

quality should be largely independent of the inlet subcooling.

There have not been many systematic studies to verify this effect. An indirect proof comes from the experiments of Styrikovich *et al.* [3]. They measured the first dryout quality firstly by changing the inlet enthalpy at constant heat flux, and secondly by changing the heat flux at constant inlet enthalpy of the working fluid. In both cases, they found about the same first dryout quality for the same heat flux, which verifies its insensitivity to the inlet subcooling. The same conclusion can be drawn from Unal's [4] experiments (see Table 1).

4.2. *Influence of system pressure*

The influence of pressure is felt mainly through the thermodynamic and physical properties of the fluid. At low pressures (relative to the critical pressure of the fluid), the density of the vapour phase is very low compared to that of the liquid phase. Other things being equal, this results in a higher superficial vapour phase velocity. This increases the entrainment rate as a result of increased interfacial shear, and the redeposition rate as a result of increased centrifugal force on the entrained droplets. Also, as the vapour phase velocity increases, the vortex of the secondary flow shifts towards the inner side [11]. This results in an increased tendency of the secondary flows in the vapour core to bring liquid from the outer side to the inner side of the coil. This should delay the occurrence of the first dryout which generally occurs on the inner side.

Thus, when the system pressure decreases, the rate of entrainment and rate of redeposition increase, and the effect of secondary flow becomes stronger. Experimental results (Fig. 4) show that the combined effect of increased redeposition and stronger secondary flow predominates over a wide range of pressures (the equivalent of 70–200 bar for water).

4.3. *Influence of coil diameter*

The major effect of the coil diameter is on the redeposition process. When the coil diameter decreases, the centrifugal force on the entrained liquid droplets increases, as does the redeposition rate. Moreover, as the centrifugal force increases, the secondary flow becomes stronger, and the centre of the vortex shifts towards the inner side. Thus, the first dryout quality

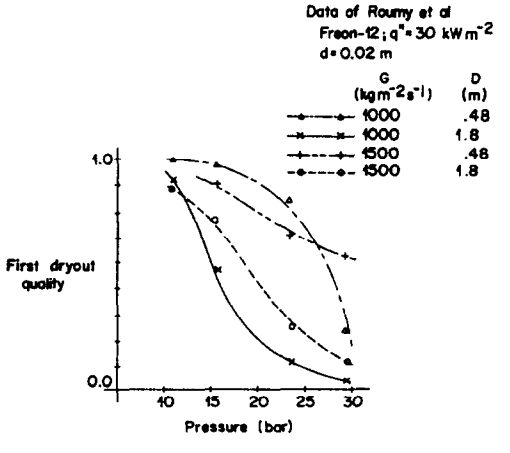

FIG. 4. Influence of pressure on the first dryout quality.

increases when the coil diameter is decreased, and it occurs more towards the inner side.

This result is in agreement with experimental data as shown in Fig. 3.

4.4. *Influence of heat flux*

By specifying the position of dryout in terms of equilibrium quality, we account for the effect of phase change on the occurrence of dryout. We assume that its effect on the secondary flow is negligible, but the presence of heat flux near the wall may generate bubbles of vapour which may give rise to additional entrainment. We may explain the observed effect (or the absence of it) of heat flux on the dryout quality through this mechanism. (The evaporation of liquid film causes an effusion of vapour from the film surface, which can have the effect of diminishing the deposition rate. However, the deposition rate in helical coils is greatly increased due to the centrifugal forces and hence the effect of effusion of vapour will be small compared to that in straight tubes, so it is neglected in the present analysis. Its effect, if any, would be to reduce the dryout quality by reducing the redeposition rate.)

In convective nucleate boiling the range of active sites for nucleation depends on the wall heat flux [13]. When the heat flux increases, this range increases, as does the number of vapour bubbles. When these bubbles leave the liquid film, they break the surface of the film, and contribute to the entrainment of the liquid. This additional entrainment, as opposed to the entrainment caused by the interfacial shear, depends on the number of bubbles leaving the surface, and hence on the wall heat flux. This may explain the decrease in the dryout quality associated with an increase in the heat flux.

The above argument also explains the relative insensibility of the first dryout quality to the heat flux in some cases. It is well established [9] that nucleate boiling is suppressed when the liquid film is not thick enough to maintain the wall superheat required for nucleate boiling. This generally happens at very high qualities. This may lead to some cases where the wall heat flux may not have any effect on the dryout quality, as explained below.

Consider the convective boiling in a uniformly-heated helical coil in which nucleate boiling is suppressed at an axial position of A, and in which dryout occurs at B (Fig. 5). This means that, between A and B, there are no entrained droplets created by the above mechanisms; all the entrainment, if any, in this region is due to the interfacial shear. If the heat flux is now increased, the point of the suppression of nucleate boiling (now A′ in Fig. 5(b)) moves downstream. If the droplets created by nucleate boiling in the region AA′ are deposited before B, the position of dryout does not change, because the heat flux has not increased the entrainment, as seen from the point of dryout. In such a case, which can occur at high redeposition rates and high qualities, heat flux does

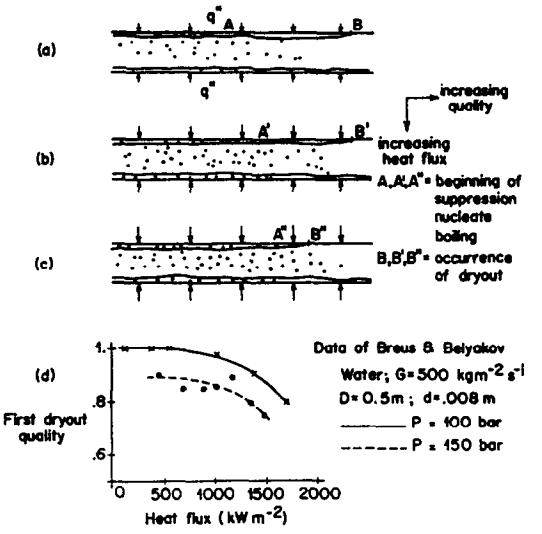

FIG. 5. The effect of heat flux on the first dryout quality. In (a), (b) and (c) only the droplets created as a result of nucleation are shown.

not affect the first dryout quality. Note that in these figures only the droplets created, if any, as a result of the presence of heat flux are shown. If the heat flux is further increased, the point of suppression of nucleate boiling (now A″ in Fig. 5(c)) moves further downstream, and the droplets created by heat flux between A and A″ may not be deposited by B. In this case, the net entrainment at point B increases, and hence the dryout occurs earlier, say at B″ such that $x(B'') < x(B)$.

To summarize, the presence of heat flux may or may not affect the first dryout quality, depending on the magnitude of the heat flux. This is shown in Fig. 5(d) where the first dryout quality is unchanged at low heat fluxes, but gradually decreases as the heat flux increases.

From the experimental results of Breus and Belyakov [6], and from those of Roumy (as presented in Fig. 4 of ref. [14]), we see that the fact that the first dryout quality is almost independent of heat flux is more valid when the pressure is low. This is consistent with the previous explanation: when the pressure decreases, the required superheat for nucleation is increased, i.e. the point A in Fig. 5 moves upstream, and hence there will be little effect of bubble-induced entrainment at the point of dryout.

4.5. *Influence of mass flux*

The mass flux has an effect on all the four mechanisms. When it is increased, the rate of entrainment increases because of increased shear, and the rate of redeposition increases because of increased centrifugal force, which also increases the secondary flow. It also has a minor effect on phase change mechanism by an increased tendency to suppress nucleate boiling. In the following, we assume that the effect of the suppression of nucleate boiling on the first dryout quality is negligible. We also assume that the rate of

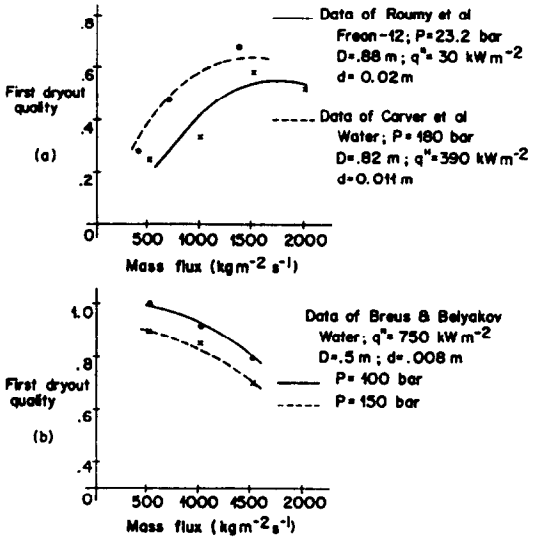

FIG. 6. Influence of mass flux on the first dryout quality. (a) In the high entrainment region. (b) In the high redeposition region.

redeposition is influenced strongly by the centrifugal force acting on the droplets. In this case, the secondary flow and the redeposition rate, both of which are functions of centrifugal force, behave in a similar manner: when one increases, the other also increases, and vice versa. Under these conditions, the film thickness, and hence the first dryout quality, can be treated as the product of two dynamic processes—entrainment and redeposition of droplets—the rate of each of which is governed by the system parameters.

The effect of mass flux on dryout quality can now be divided into two zones corresponding to large and small rates of redeposition as compared to the rate of entrainment. In the case of large redeposition rates, the equilibrium value is governed by the slower entrainment process. Thus, an increase in the rate of entrainment, caused by an increase in the mass flux, will have more effect on the dryout quality than a corresponding increase in the redeposition rate. In other words, $\Delta(R_e)/R_e > \Delta(R_d)/R_d$, where R_e and R_d are the rates of entrainment and redeposition, and $\Delta(R_e)$ and $\Delta(R_d)$ are the increase in their rates caused by an increase in the mass flux. As a result, the first dryout quality decreases. Similarly, when R_d is much less than R_e, the slower process of redeposition determines the value of the first dryout quality. In this case, $\Delta(R_e)/R_e < \Delta(R_d)/R_d$. Thus, the dryout quality increases when mass flux is increased.

It remains to identify these two zones. Since the rate of redeposition is determined mainly by the centrifugal force, the case of small redeposition rate can be found when the coil diameter is large and the system pressure is high (high gas density and low slip ratio). For this combination, the dryout quality increases as mass flux increases. This is shown in Fig. 6(a). The case of large redeposition rate occurs for small coil diameter and low system pressure. Here the dryout quality decreases when the mass flux increases, as shown in Fig. 6(b).

Until now, we have been treating dryout as a consequence of hydrodynamic effects in well established annular flow. This may not be the case when it occurs at very low qualities for heat fluxes much less than those required for the CHF condition by other mechanisms such as vapour blanketing. This low-quality dryout is due mainly to the effect of stratification. This is evident from the conditions in which it takes place in general: low mass flux, large coil diameter and high (relative) pressure. Each of these leads to weak secondary flows in the coil, and as a result, the flow is stratified, with the film thickness distribution being similar to that shown in Fig. 2(a). The stratification of flow has a direct effect on the dryout mechanism: since the film is very thin at the top, very little liquid is removed from these by entrainment. Similarly, since the secondary flow is weak, there is very little replenishment of the liquid at the top. Thus, dryout occurs mainly as a result of draining and evaporation of the liquid film at the top; entrainment and redeposition mechanisms play only a minor role. The very first dryout quality shows great sensitivity to system parameters. Increased coil diameter or reduced mass flux decrease it by making the film flow rate much less at the top. An increase in heat flux also decreases it, the thinner liquid film at the top being evaporated early.

5. QUANTITATIVE CHARACTERIZATION OF DRYOUT

The arguments of the above section show the possibility of grouping data into 'zones of dominance', which can then be correlated using statistical techniques. In this section, we use this method to develop correlations for the quantities specified in Section 2. The experimental data used in this study were pooled from those available from publications and reports. The range of parameters and the number of data points in each source are listed in Table 2.

5.1. *First dryout quality*

It is well known that the first dryout quality is very sensitive to system parameters. The data are in general very difficult to correlate with the result that some researchers [5–7] have tried to classify them into groups. But such division has generally been arbitrary and/or requires a priori the knowledge as to which group the data belong to. For example, Breus and Belyakov [6] present two correlations for two sets of dryout data, but do not indicate how to select either of the two. Both Jensen [5] and Tomita *et al.* [7] have divided their data in Freon-113 and water respectively into two groups, and developed separate correlations for each group. However, their correlations do not predict the data of Roumy [1] (working fluid: Freon-12), and of Breus and Belyakov [6] (working fluid: water) respectively, within the range of validity of these correlations. We argue that the reason for this

Table 2. Experimental data for first dryout quality

No.	Source	Fluid	P (bar)		D (m)	d (m)	G (kg m^{-2} s^{-1})	q" (kW m^{-2})	Method of heating	Number of data
1	Roumy [1]	R-12	11	19.4	0.133	0.02	500	10	electric	103
			15.5	12.5	0.48		1000	20		
			23.2	7.05	0.88		1500	30		
			28.1	5.12	1.8		2000	40		
2	Styrikovich *et al.* [3]	water	100	12.4	0.136	0.008	500	200	electric	17
			177	4.32	0.136		1000	to		
							1500	1800		
3	Unal [4]	water	150	6.29	0.7	0.018	100	50	liquid	96
			177	4.32	1.5		to	to	metal	
			200	2.86			1500	700		
4	Breus and Belyakov [6]	water	100	12.4	0.08	0.008	500	200	electric	172
			150	6.29	0.30		1000	to		
			200	2.86	0.50		1500	1800		
5	Carver *et al.* [8]	water	177	4.32	0.82	0.011	380	220	electric	25
					3.3		675	to		
							1350	700		
							1900			
								Total		413

is the rather arbitrary classification of data, and that the degree of arbitrariness can be reduced to some extent by using the qualitative explanations of the above section.

The discussion in the previous section provides the basis for a classification of data in terms of factors which determine when dryout occurs. We propose three such factors which dictate the occurrence of dryout for a given combination of system parameters.

(a) Stratification: the combination of high relative pressure, low mass flux and large coil diameter leads to a stratified flow, and to low dryout qualities.

(b) Redeposition: the combination of low relative pressures, small coil diameters and high mass fluxes leads to an annular flow with a large redeposition rate, and to very high dryout qualities.

(c) Entrainment: the combination of very high mass flux but relatively large coil diameters leads to a case of high entrainment but a relatively lower redeposition rate; as a result, the dryout quality is neither low nor high.

Using a large set of experimental data over a wide range of parameters, one can develop a 'dryout map' in which data can be sorted into groups each belonging to a zone in which one (or more) of these effects dominates. We have used the data shown in Table 2 to identify these zones on one- and two-dimensional maps using non-dimensional groups to represent the dominating effects. On an ideal map, one would expect the data to fall into groups of low quality dryout and high quality dryout, etc., the grouping being with the above reasoning. Of all the maps that we tried, we found this requirement best met by the map shown in Fig. 7. It has two dimensionless groups as coordinates. Its x-coordinate, the group $x_0 = G/(\rho_v\sqrt{(gD)})$, is a measure of the centrifugal force acting on the gas phase as well as on the entrained droplets, and this is important in the redeposition process. Similarly, the y-coordinate is the liquid Reynolds number modified by a correction factor for the tube diameter; it is defined as

$$y_0 = G \cdot d^*/\mu_l = G \cdot d \cdot (d/0.02)^{1/2}/\mu_l$$

and is important in characterizing the entrainment process. It is to be noted that the tube diameter correction factor used here is the same as that suggested [15] for straight tubes.

We readily identify the three zones of dominance on this map in the following manner. The gravity-affected zone (low G and high D, and hence small x_0

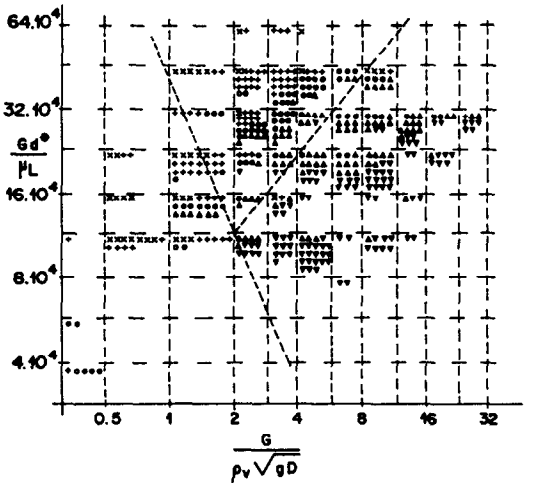

FIG. 7. Experimental data of first dryout quality on a 'correlation map'. The first dryout quality is discretized as follows: ×, $0 \leqslant x_1 < 0.25$; +, $0.25 \leqslant x_1 < 0.45$; ○, $0.45 \leqslant x_1 < 0.65$; △, $0.65 \leqslant x_1 < 0.85$; ▽, $0.85 \leqslant x_1 < 1$.

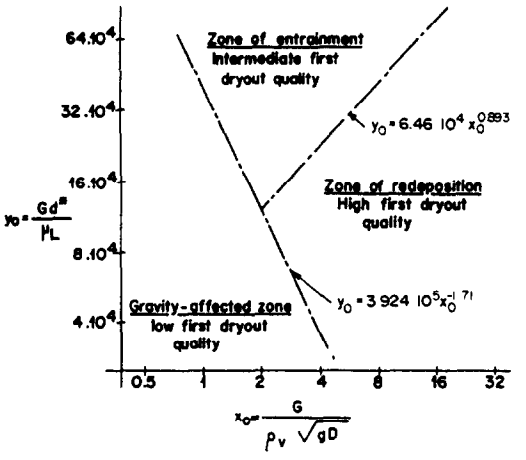

FIG. 8. Zones of dominance of dryout in helical coils.

and small y_0 lies towards the bottom left corner of the map, where we find a concentration of low dryout quality points. The redeposition-dominated zone (large centrifugal force, and so large x_0) lies towards the right hand side of the map, where we find many high dryout quality points. The entrainment-limited zone (high G, and so large y_0) lies on the upper side of the map, where the dryout quality is generally neither low nor high. We also note that as the redeposition increases (moving horizontally from left to right), the dryout quality increases, and as the entrainment increases (moving vertically up), the dryout quality decreases. Both these trends are compatible with what is expected.

Figure 8 shows the demarcation of these three zones. The criteria for this demarcation were (i) that they should be consistent with physical arguments (see the above paragraph) and (ii) that they should lead to a better prediction of the data. In view of the paucity of data, these lines of transition must be treated as tentative. Using regression analysis, the following correlations were developed for each zone in terms of dimensionless groups.

Gravity-dominated zone

$$x_1 = 10^{7.068}\left(\frac{\rho_l}{\rho_v}\right)^{-2.378}\left(\frac{Gd}{\mu_l}\right)^{-1.712} \times \left(\frac{G}{\rho_v\sqrt{(gD)}}\right)^{0.967}\left(\frac{q''}{G\lambda}\right)^{-0.740}. \quad (1)$$

Redeposition-dominated zone

$$x_1 = 3.223 + \log_{10}\left[\left(\frac{\rho_l}{\rho_v}\right)^{0.101} \times \left(\frac{Gd}{\mu_l}\right)^{-0.785}\left(\frac{G}{\rho_v\sqrt{(gD)}}\right)^{0.067}\left(\frac{q''}{G\lambda}\right)^{-0.43} \times \left(\frac{q''}{\mu_l\lambda}\sqrt{\left(\frac{\sigma}{g(\rho_l-\rho_v)}\right)}\right)^{0.098}\right]. \quad (2)$$

Entrainment-dominated zone

$$x_1 = 10^{3.235}\left(\frac{\rho_l}{\rho_v}\right)^{-0.267}\left(\frac{Gd}{\mu_l}\right)^{-0.984}\left(\frac{G}{\rho_v\sqrt{(gD)}}\right)^{0.950} \times \left(\frac{q''}{G\lambda}\right)^{-0.428}\left(\frac{q''}{\mu_l\lambda}\sqrt{\left(\frac{\sigma}{g(\rho_l-\rho_v)}\right)}\right)^{0.119}. \quad (3)$$

It is to be noted that the tube diameter used in the above correlations is not the modified one; the use of d^* instead of d would only change one of the constants because d and d^* are perfectly correlated statistically. This emphasizes the empirical nature of the correlations: they do not explicitly model any of the mechanisms discussed above. This is not surprising because very little is known about these mechanisms in helical coils (or for that matter in horizontal tubes, which can perhaps be extended to helical coils). For example, while it is generally agreed that the rate of redeposition in coils is higher than in straight tubes, the increase is yet to be quantified. Similarly, no correlations are available for the rate of entrainment in annular flow when the film thickness varies around the circumference (as in horizontal tubes and helical coils). For this reason, one can use only qualitative arguments to reduce arbitrariness in developing a predictive correlation applicable to a wide range of parameters. The selection of a particular non-dimensional group for correlation was based on the coefficient of correlation between the group and the dryout quality and on the need for bringing together data of different fluids. Similarly, the form of the correlation depended mainly on how well a particular form correlated the data in a zone. Thus, the demarcation of zones and the correlation of data were carried out in an iterative manner, although no optimization techniques were used.

The comparison between the actual and the predicted first dryout quality is shown in Fig. 9. We find that most of the 400-odd points lie within an absolute error band of ± 0.20. In view of the fact that the data used in this study were obtained from different sources using different experimental methods and different criteria for the detection of dryout, and that it was sensitive to many system parameters, especially at low dryout qualities, we consider the prediction to be very good. We note here that the correlations are valid over a wide range of parameters (see Table 2), and that they are applicable for at least two fluids—water and Freon-12.

5.2. *Partial dryout region*

In this section, we develop empirical correlations for the quality at total dryout of the tube, the circumferential propagation of partial dryout, and the length of the partial dryout region. It should be noted that we have assumed complete thermodynamic equilibrium between the two phases in the partial dryout region. Thus, the quality referred to in this section and its correlations is the equilibrium quality and not the actual quality. This assumption should be borne in mind in employing these results.

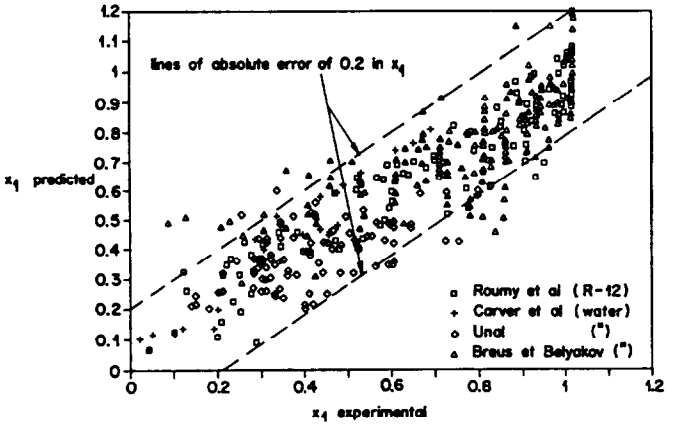

FIG. 9. Comparison between experimental and predicted values of the first dryout quality.

5.2.1. *Total (last) dryout quality.* There have been comparatively fewer studies and correlations to determine the total dryout quality. It has generally been observed that the total dryout of the tube occurs for an equilibrium quality of around unity. Such high total dryout qualities are not unexpected because of the increased and preferential redeposition rate in coils. Using the experimental data shown in Table 3, we have developed the following correlation for the total dryout quality in terms of dimensionless groups:

$$x_{tot} = \log_{10}\left[\left(\frac{\rho_l}{\rho_v}\right)^{-1.61}\left(\frac{\mu_l}{\mu_v}\right)^{1.722}\left(\frac{Gd}{\mu_l}\right)^{0.494} \times \left(\frac{G^2 d}{\sigma\rho_l}\right)^{-0.381}\left(\frac{G}{\rho_v\sqrt{(gD)}}\right)^{0.08}\right]. \quad (4)$$

Figure 10 shows the comparison between the actual and the predicted values of the total dryout quality. The excellent agreement between the two is primarily due to the fact that the total dryout quality is not very sensitive to system parameters.

5.2.2. *Circumferential propagation of dryout.* There have been very few (only two, to the best of our knowledge, those of Carver *et al.* [8] and Roumy [1]) systematic measurements of partial dryout qualities. Assuming thermodynamic equilibrium, it has been shown [2] that the circumferential propagation of the dryout front can be described in terms of two normalized parameters, namely the non-dimensionalized partial dryout quality, δx, defined as $\delta x = (x - x_l)/(x_{tot} - x_l)$, and the fraction of wetted parameter, f_w, defined as f_w = (wetted perimeter of the tube)/total perimeter of the tube. The functional relationship between these two in the partial dryout region can be represented by a curve. Figure 11 shows this curve based on the data of Roumy [1]. He used Freon-12 as the working fluid and measured the wall temperature at eight circumferential positions.

Thus, for each combination of P, D, G and q'', the quality at which dryout occurs at each of the eight circumferential locations can be determined. Assuming that one-eighth of the tube perimeter is dried out when one thermocouple shows dryout, and one-quarter is dried out when two of the eight show dryout, etc., a curve between δx and f_w can be drawn for each run. Figures 12(a)–(d) show the average of these curves as a function of heat flux, coil diameter, mass flux and system pressure. It can be seen that the

Table 3. Experimental data for total dryout quality

No.	Source	Fluid	P(bar)		D (m)	d (m)	G (kg m^{-2} s^{-1})	q'' (kW m^{-2})	Method of heating	Number of data
1	Roumy [1]	R-12	11	19.4	0.133	0.02	500	10	electric	93
			15.5	12.5	0.48		1000	20		
			23.2	7.05	0.88		1500	30		
			28.1	5.12	1.8		2000	40		
2	Unal [4]	water	150	6.29	0.7	0.018	100	50	liquid	36
			177	4.32			to	to	metal	
			200	2.86			1500	700		
3	Carver *et al.* [8]	water	177	4.32	0.82	0.011	380	220	electric	17
					3.3		675	to		
							1350	700		
							1900			
								Total		146

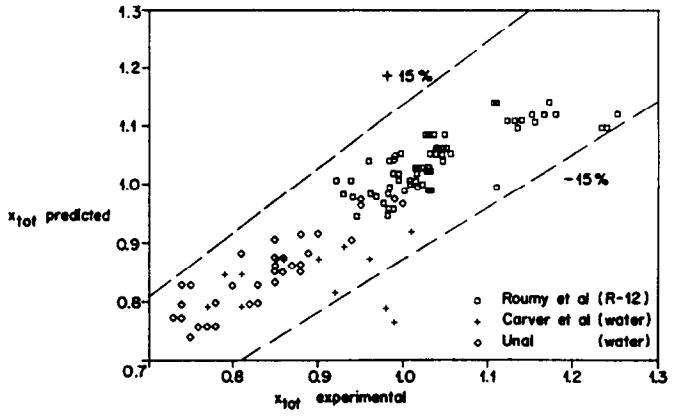

FIG. 10. Comparison between experimental and predicted values of x_{tot}.

curve is not a strong function of heat flux or coil diameter. (The curve corresponding to a diameter of 0.133 m is subject to large errors in the determination of δx because there is little difference between x_1 and x_{tot}.) Similarly, the curve is independent of the mass flux except at low mass fluxes where stratification may occur. In view of this, we give two correlations (see Table 4) for the quality in the partial dryout region, one for the gravity-dominated zone and the other for other zones. These correlations are based on the data at high pressures (Table 2).

Table 4 also gives the reciprocal correlations, i.e. the fraction of wetted perimeter as a function of the non-dimensionalized quality in the partial dryout region. Using these curves, along with the correlations for the first and the total dryout quality, one can determine the quality for a given fraction of wetted perimeter and vice versa. In other words, one can answer the question: what is the quality at which, say, one-third of the tube is dried out?

We have already discussed the variation of film thickness around the tube and its importance in determining the angular position of the first dryout. From our discussion above, we conclude that the first dryout occurs near the upper part of the tube for gravity-affected dryout, whereas it occurs more towards the inner side in the other regions. (Note that this is valid for non-inverted annular flow, which prevails at relatively high pressures; the minimum pressure covered in this study is a water-equivalent of 70 bar.) Also, the spread of dryout is nearly symmetric about a diametrical plane passing through the point of the first dryout, as shown in Fig. 3. We can use this information with the rest in this section to answer the question: what part of the tube is still wetted at such and such quality?

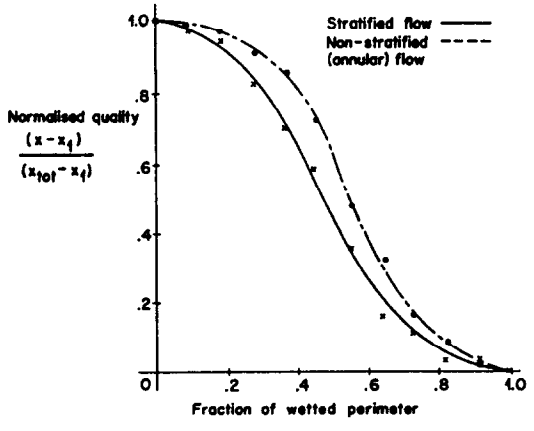

FIG. 11. Characteristic relation between normalized quality and the fraction of wetted perimeter in the region of partial dryout.

This will be clear from the following example. For a given set of system parameters, namely fluid properties G, D, d and q'', we can determine which effect dominates the occurrence of dryout. Suppose the combination of parameters lies in the redeposition zone. Then we can find out the first dryout quality (x_1) and the total dryout quality (x_{tot}) from correlations (2) and (4), respectively. Since by assumption, the global system parameters indicate a redeposition-dominated dryout (Fig. 8), we also know that dryout starts near the inner side of the tube, say at $\theta_1 = 300°$. Using the correlations in Table 4, we can then find for any quality between x_1 and x_{tot} a corresponding fraction of wetted perimeter. Let this be 0.6 for a given δx. This means that 40% of the perimeter, corresponding to an arc of 144°, is dried out, and that its angular position is given by

$$(\theta_1 - 144/2) < \theta_d < (\theta_1 + 144/2).$$

This is shown in Fig. 13.

5.2.3. *Length of the partial dryout region* (Δz). The partial dryout region can be very long if dryout starts at a low quality. Knowing the first and the total dryout (equilibrium) qualities, we can estimate the length (Δz) of this region from an energy balance

$$\int_{z_1}^{z_{tot}} q''_{pw} \cdot \pi d \cdot dz = G \cdot \lambda \cdot \pi d^2/4 \cdot (x_{tot} - x_1). \quad (5)$$

In the case of a heat flux-imposed system, q'' is known explicitly, and Δz can easily be determined by analytical or numerical integration. In the case of constant wall heat flux, q'', it is given by

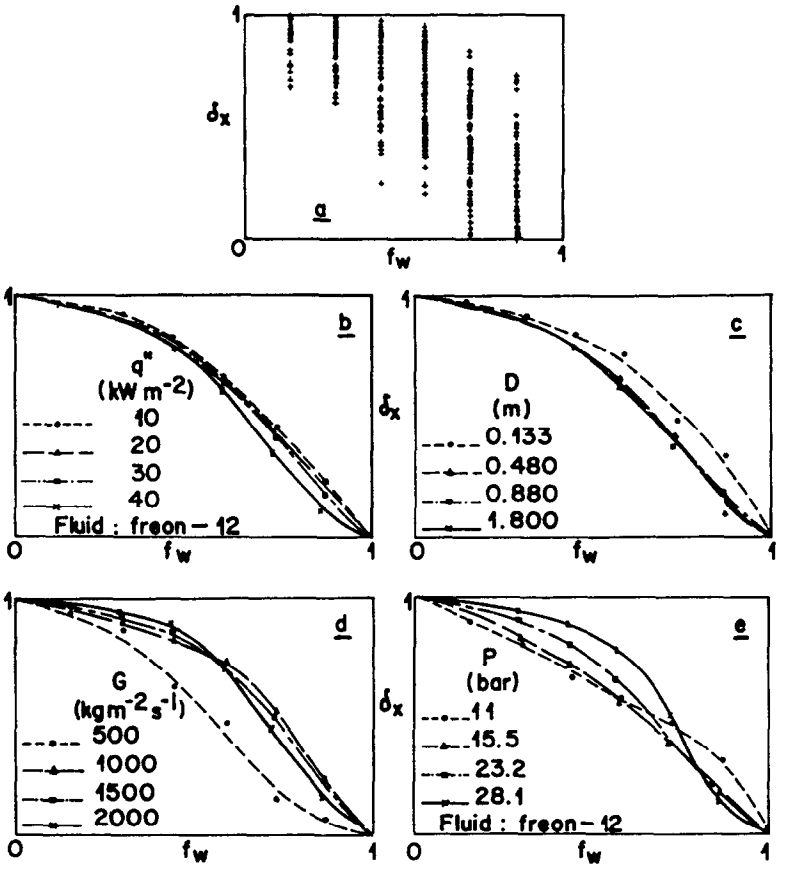

FIG. 12. Circumferential propagation of dryout characteristic: relation between δx and f_w for Roumy's results. (a) For all the data. (b) Parameter q''. (c) Parameter D. (d) Parameter G. (e) Parameter P.

$$\Delta z = G \cdot d \cdot \lambda / (4 \cdot q''). \quad (6)$$

For a temperature difference-imposed system, the wall heat flux depends on the overall heat transfer coefficient between the 'tube side' and the 'shell side', and also on the occurrence or not of local dryout. In this case, one can use the correlations of the previous sections to develop a 'two-fluid model' to determine the length of the partial dryout region, as discussed in ref. [14].

6. CONCLUSIONS

In this paper, we have used the results obtained by various research laboratories including experiments done at the Nuclear Research Centre at Grenoble to determine the effect of pressure, coil diameter, mass flux and heat flux on the dryout quality. We have shown that the effect of a parameter can be predicted qualitatively by considering its effect on (a) entrainment of the liquid, (b) redeposition of the droplet, (c)

Table 4. Constants in the polynomial correlations between δx and f_w

	Gravity-affected dryout		Dryout in the non-stratified zones	
	Form of correlation		Form of correlation	
j	$\delta x = \Sigma_j a_j f_w^j$	$f_w = \Sigma_j b_j \delta x^j$	$\delta x = \Sigma_j a_j' f_w^j$	$f_w = \Sigma_j b_j' \delta x^j$
0	1.003	0.992	1.006	0.993
1	−0.804	−4.163	−1.055	−2.871
2	5.691	17.57	9.624	11.37
3	−26.59	−37.80	−34.55	−26.81
4	−35.06	37.51	40.00	30.29
5	−14.36	−14.12	−15.02	−12.95

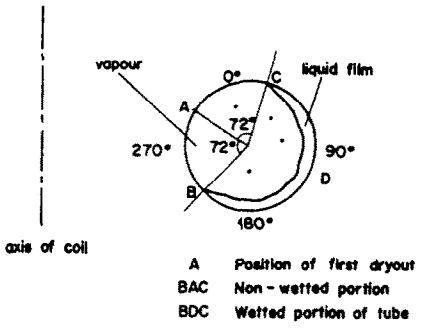

FIG. 13. Cross-section of the tube for $f_w = 0.6$; dryout begins at point A, towards the inner side.

secondary flow and (d) phase change resulting from surface heat flux. It is argued that this interpretation provides the basis for the classification of dryout data into zones dominated by the phenomena of stratification, redeposition and entrainment. Using experimental data, a two-dimensional map has been developed in which these three zones are identified. Empirical correlations are given for the first dryout quality in each zone.

We have also presented a characterization of the partial dryout region. Correlations are given for the total dryout quality and for the circumferential propagation of the dryout front.

REFERENCES

1. R. Roumy, Dryout in helically coiled tubes with boiling Freon-12, European Two-phase Group Meeting, Risp (1971).
2. S. Jayanti, Contribution à l'étude de l'assechement en hélices, Memoire de D.E.A., Institut National Polytechnique de Grenoble, France (1987).
3. M. A. Styrikovich, V S. Polonsky and V. Vreshetov, Experimental investigation of the critical heat flux and post-dryout temperature regime of helical coils, *Int. J Heat Mass Transfer* **27**, 1245–1250 (1984).
4. H. C. Unal, Some aspects of two-phase flow, heat transfer and dynamic instabilities in medium- and high-pressure steam generators, Thesis for "Doctor in de Technische" of The Netherlands (1981).
5. M. K. Jensen, Boiling heat transfer and critical heat flux in helical coils, Ph.D. Thesis, Iowa State University, U.S.A. (1980).
6. V. I. Breus and I. I. Belyakov, Burnout in helical coils at high pressures, *Thermal Engng* **30**(10), 592–593 (1983).
7. Y. Tomita, T. Kosugi, J. Kutoba, F. Nakajima and T. Tschuiya, Dryout in sodium-heated helically-coiled steam generator tubes. In *Liquid Metal Engineering and Technology*, pp. 189–194. BNES, London (1984).
8. J. R. Carver, C. R. Kakarala and J. S. Slotnik, Heat transfer in coiled tube with two-phase flow, Babcock and Wilcox Company Research Report No. 4438 (1964)
9. J. G. Collier, *Convective Boiling and Condensation* (2nd Edn). McGraw-Hill, New York (1981).
10. G. F. Hewitt, *Two-phase Flow and Heat Transfer in the Power and Process Industries* (Edited by A. E. Bergles, J. G. Collier, J. M. Delhaye, G. F. Hewitt and F Mayinger), Chap. 9. Hemisphere, Washington, DC (1981).
11. W. Y. Soh and S. A. Berger, Fully developed flow in a curved pipe of arbitrary curvature ratio, *Int. J Numer Meth. Fluids* **7**, 733–755 (1987).
12. S. Banerjee, E. Rhodes and D. S. Scott, Studies on cocurrent gas–liquid flow in helically coiled tubes, *Can. J Chem. Engng* **47**, 445–453 (1969).
13. W. M. Rohsenow and J. P. Hartnett, *Fundamentals of Heat Transfer*, Chap. 2. McGraw-Hill, New York (1973).
14. S. Jayanti and G. Berthoud, Dryout in helical coils, *Third Int. Topical Meeting on Nuclear Power Plant Thermal Hydraulics and Operations*, Paper No. A2.A-4, Seoul, South Korea, 14–17 November (1988).
15. Working Party of the Heat and Mass Transfer Section of the Scientific Council of the U.S.S.R. Academy of Sciences, Tabular data for calculating burnout when boiling water in uniformly heated round tubes, *Teploenergetika* **23**(9), 90–92 (1976).

CARACTERISATION DE L'ASSECHEMENT DANS UN TUBE HELICOIDAL

Résumé—La connaissance du phénomène d'assèchement dans un tube hélicoïdal est importante pour l'étude des générateurs de vapeur de certains réacteurs à neutrons rapides. Il est apparu nécessaire d'améliorer la prédiction du point d'apparition de l'assèchement ainsi que le traitement de la zone d'assèchement partiel. Dans cet article, nous présentons une analyse qualitative des données qui nous permet ensuite de classer celles-ci en trois familles différentes: les données pour lesquelles l'assèchement est gouverné par les phénomènes de stratification, celles pour lesquelles l'assèchement est dominé par les phénomènes de redéposition et celles pour lesquelles ce sont les phénomènes d'entraînement qui dominent. A partir de cette analyse, nous séparons alors les différentes données en notre possession pour fournir une carte d'assèchement. Des corrélations pour chaque famille sont ensuite présentées ainsi qu'un traitement de la zone d'assèchement partiel.

BESCHREIBUNG DES "DRYOUT" IN SPIRALROHRWÄRMETAUSCHERN

Zusammenfassung—Zur genauen Auslegung von LMFBR-Dampferzeugern ist die Kenntnis über das Auftreten eines "Dryout" in Spiralrohrwärmetauschern wichtig. Die bisherigen Untersuchungen dieses Problems sind nicht befriedigend, sowohl in der Berechnung des Dampfgehaltes des ersten "Dryouts", als auch in der Behandlung des partiellen "Dryout"-Gebietes. Es werden qualitative Argumente vorgebracht, um zu zeigen, daß "Dryout" aufgrund unterschiedlicher Gegebenheiten entstehen kann: durch Schichtung, durch *Re*-Deposition oder durch "Entrainment". Ergebnisse aus verschiedenen Laboratorien einschließlich der Experimente von CENG in Grenoble werden verwendet, um Übergangskriterien für diese Gebiete in einer "Dryout"-Karte zu entwickeln. Für den "Dryout"-Dampfgehalt in jeder Gruppe werden Korrelationen angegeben. Schließlich wird eine Analyse des partiellen "Dryout" vorgestellt.

ХАРАКТЕРИСТИКА КРИЗИСА ТЕПЛОПЕРЕНОСА В СПИРАЛЬНОЙ КАТУШКЕ

Аннотация—Определение кризиса теплопереноса в спиральных катушках существенно для правильного конструирования паровых генераторов некоторых LMFBR. Результаты, полученные в этой области ранее, не являются удовлетворительными для предсказания первого кризиса теплопереноса или для исследования участка с частичным кризисом. Представленные качественные данные показывают, что при кризисе теплопереноса могут преобладать стратификация, вторичное осаждение и унос. С целью разработки переходных критериев для этих зон на "карте кризиса" используются результаты, полученные различными лабораториями, в том числе и в CENG, Гренобль. Даны соотношения для определения степени кризиса теплообмена в каждой группе. Анализируется также область с частичным кризисом.